ACS APPLIED MATERIALS & INTERFACES

Research Article

www.acsami.org

Effects of Lithium Niobate Polarization on Cell Adhesion and Morphology

Valentina Marchesano,[†] Oriella Gennari,[†] Laura Mecozzi,[†,‡] Simonetta Grilli,[*,†] and Pietro Ferraro[†]

[†]National Council of Research, Institute of Applied Science & Intelligent Systems (ISASI) 'E. Caianiello', Via Campi Flegrei 34, 80078 Pozzuoli (NA), Italy

[‡]University "Federico II", P. le Tecchio 80, 80125 Napoli, Italy

ABSTRACT: Understanding how the interfacial effects influence cell adhesion and morphology is of fundamental interest for controlling function, growth, and movement of cells *in vitro* and *in vivo*. In particular, the influence of surface charges is well-known but still controversial, especially when new functional materials and methods are introduced. Here, the influence of the spontaneous polarization of ferroelectric lithium niobate (LN) on the adhesion properties of fibroblast cells is investigated. The spontaneous polarization of LN has one of the largest known magnitudes at room temperature (~78 μC/cm^2), and its orientation can be patterned easily by an external voltage, this motivating highly the investigation of its interaction with cells. Immunofluorescence and migration assays show strong evidence that the surface polarity regulates the adhesion functions, with enhanced spreading of the cytoskeleton on the negative face. The results suggest the potential of LN as a platform for investigating the role of charges on cellular processes, thus favoring new strategies in fabricating those biocompatible constructs used for tissue engineering. In fact, the orientation of the high-magnitude polarization can be patterned easily and, in combination with piezoelectric, pyroelectric, and photorefractive properties, may open the route to more sophisticated charge templates for modulating the cell response.

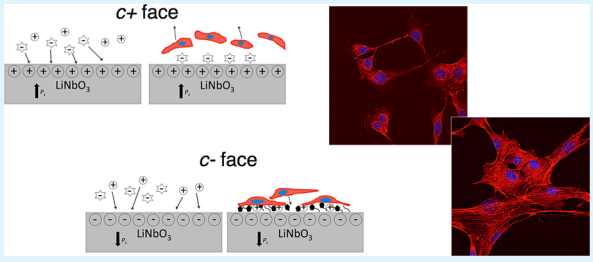

KEYWORDS: *cell adhesion, lithium niobate, cytoskeleton, ferroelectrics, stress fibers*

INTRODUCTION

The interaction of cells with nonbiological materials is crucial for controlling cell function, growth, and movement, in both *in vitro* and *in vivo* environments, thus providing the criteria for designing those biocompatible materials used for engineering biohybrid organs.[1−6] In fact, it is well-known that, during the implantation of such devices, the material surface is exposed to numerous proteins present in blood, interstitial fluids, and damaged extracellular matrix (ECM), resulting in the formation of a complex layer of adsorbed proteins at the material surface.[7] Some of these proteins contain specific amino acid sequences that bind to cell surface integrin receptors, thus influencing cell behavior and gene expression.[8] Recently, a wide variety of materials demonstrating how the physicochemical properties of the material influence the protein adsorption and therefore the cell response have been studied. Some of these works focus their attention on the interaction of cells with nanoparticles,[9−11] while others investigate the effect of hydrophobicity[12,13] or the surface potential in specific substrates,[14] just to cite some. In particular, in the past several decades, there have been many developments in the so-called field of "bioceramics", and Baxter and co-workers published an excellent review on this topic.[15] The electric potentials, which occur in bones under mechanical loading, are explained partially in terms of the piezoelectric properties of the collagen.[16] These potentials have been linked to the mechanical adaptation of bones in response to loading,[17,18] thus suggesting that the addition of an electrically active component to an implant material may improve healing and adaptation of the surrounding tissue. Consequently, the level of interest in bioinspired research that aims to understand if and how polarization of piezoelectric ceramics can improve the response of cells that synthesize bones (osteoblasts) to artificial implants and grafts has increased.[19−24] However, new biocompatible platforms are always being sought to understand how materials with different surface properties may influence and control the cellular response, thus leading to the development of principles that can be used for engineering useful implantable devices and tissue-engineered constructs. In this framework, ferroelectric crystals may have great potential, because of their unique polarization effect, with a relatively high spontaneous polarization that can be switched by an external electric field, because of their inherent ability to sustain a charged surface in a variety of environments.[25] In particular, LN, with a value of ~78 μC/cm^2, has one of the largest polarization magnitudes known at room temperature, and is easily reversible for modulating the surface charge polarity. LN is well-known in the field of electro-optics, but its influence on living cells has been neglected. Some works have dealt with the interaction and assembly of molecules and particles with the modified surface of ferroelectric thin films or crystals.[26−29] However, to the best of our knowledge, only very

Received: June 16, 2015
Accepted: July 29, 2015
Published: July 29, 2015

DOI: 10.1021/acsami.5b05340
ACS Appl. Mater. Interfaces 2015, 7, 18113−18119

recently has the biocompatibility of LN and lithium tantalate (LT) been investigated for the first time,[30] and a couple of works on the response of cells cultured onto the surface of ferroelectric bulk crystals have been published. Carville et al. studied the interaction of osteoblast cells with the surface of LN crystals, concluding that the surface charge promotes the cell attachment, proliferation, and function, regardless of the polarization sign.[31] Moreover, they present controversial results of cell proliferation, compared to previous studies performed with bioceramics.[15] Christophis et al. investigated the adhesion of fibroblast cells onto periodically poled LT crystals functionalized by a protein-based coating.[32] They concluded that cells tend to orient their nucleus, avoiding the positions of high field gradients, but without any evident influence of the polarization sign on cell adhesion. In this poor framework, it is clear that the matter is at a very preliminary and controversial stage.

Here, we investigate the interaction of living NIH-3T3 mouse embryonic fibroblast cells with the surface of *c*-cut polished crystals of LN not only by observing the proliferation of the cells but also by focusing attention, for the first time, on the effects of the polarization sign on the cytoskeleton and focal adhesion organization that, in turn, regulates a wide variety of cell functions such as cell migration and fate. Immunofluorescence and wound healing assays have been performed on cells plated on surfaces with opposite polarities, and the results show a remarkable relationship of cell morphology and migration with polarization sign, thus throwing light on the controversial subject. The results appear also to be in agreement with the interpretations provided in the case of osteoblasts joined to ceramics.[15]

EXPERIMENTAL SECTION

Lithium Niobate Crystal Samples. LN is a human-made dielectric that does not exist in nature. It is a rhombohedral crystal that, at room temperature, belongs to the 3*m* group and consists of planar sheets of oxygen atoms in a distorted hexagonal close-packed configuration.[33] Octahedral interstices are formed, one-third of which is occupied by niobium (Nb) atoms, one-third is occupied by lithium (Li) atoms, and the rest is vacant. Above the Curie temperature, T_c (around 1210 °C), the phase is paraelectric (no spontaneous polarization), while in the ferroelectric phase, below the T_c, LN exhibits spontaneous polarization P_s along the *c* axis, resulting in a *c*+ face and a *c*− face. The *c*+ face corresponds to the positive end of the dipole, and the *c*− face corresponds to the negative end of the dipole. In this work, we used *c*-cut LN crystal samples 500 μm thick and 2 cm × 2 cm large, cut out from single-domain wafers 3 in. in diameter and polished optically on both faces (purchased from Crystal Technology, Inc.).

***In Vitro* Cell Culture.** The cell adhesion on the LN crystal samples was evaluated *in vitro* using mouse embryonic fibroblast cells (NIH-3T3). Cells were grown in Petri dishes in Dulbecco's modified Eagle's medium (DMEM) containing 4.5 g/L D-glucose and supplemented with 10% FBS (fetal bovine serum), 100 units/mL penicillin, and 100 μg/mL streptomycin. Subsequently, they were harvested from the tissue culture flasks by incubation with a 0.05% trypsin/EDTA solution for 5 min. The cells were then centrifuged, resuspended in a complete medium, and then seeded on eight LN crystal substrates at a density of 1×10^5 cells/mL; NIH-3T3 cells were then incubated in conventional 50 mm diameter Petri dishes at 37 °C under a humidified 5% CO_2 atmosphere. Half of the substrates exposed the *c*− face, while the other exposed the *c*+ face. Cell adhesion and spreading were observed over 24 h under a standard inverted optical microscope (AxioVert, Carl Zeiss, Jena, Germany).

Biocompatibility Assay. The biocompatibility of LN was tested quantitatively by using a conventional live/dead viability/cytotoxicity assay kit (Molecular Probes Invitrogen). The cells were seeded at a density of 1×10^5 cells on three kinds of substrates, LN (*c*−), LN (*c*+), and sterile glass, which was used as a control (Delchimica Scientific Glassware),[34] and were incubated in Petri dishes for 24 and 48 h. After incubation, 1 mL of the combined live/dead cell staining solution (2 μM calcein AM and 4 μM EthD-1 in D-PBS) was added to the dish and incubated for 45 min at room temperature. The kit contains calcein-AM, which stains live cells as green, and the ethidium homodimer, which stains the dead cells as red. Samples were then observed under a conventional fluorescence upright microscope (Axio Imager, Carl Zeiss). To evaluate the proliferation rate, cells were harvested by incubation with a 0.05% trypsin/EDTA solution for 5 min and counted with a conventional Burker's chamber.

Immunofluorescence. The cells were seeded on *c*−, *c*+, and glass as a control and incubated for 48 h. After incubation, the medium was aspirated and the samples were rinsed with a phosphate-buffered saline (PBS) solution and fixed in 4% paraformaldehyde in PBS (pH 7.4) for 10 min at room temperature. The samples were then washed in PBS and permeabilized with 0.1% Triton X-100 in PBS for 5 min and a blocking solution (1% BSA in PBS) for 30 min. The nuclei were stained with blue fluorescent Hoechst 33342 dye, trihydrochloride, trihydrate (Molecular Probes Invitrogen) to reach a final concentration of 5 μg/mL, and the actin was stained with the tetramethylrhodamine (TRITC)-conjugated phalloidin to reveal the cytoskeleton network. Fluorescent phalloidin is widely used in the study of actin networks in biology. Supplementary immunostaining with antivinculin antibody was conducted to visualize further the actin-based cytoskeleton in the cell−cell and cell−substrate junctions.[34,35] The cells were incubated first in primary antivinculin antibody (Biorbyt Limited) diluted in blocking solution for 1 h and then in secondary donkey anti-rabbit DyLight 488 (Thermo Scientific) at a 1:200 dilution in a blocking buffer solution for 45 min. For double labeling, the TRITC-conjugated phalloidin was incubated simultaneously with the secondary antibody. The crystals were washed three times in PBS between each antibody treatment. After being permeabilized and stained, the samples were rinsed for 5 min three times in PBS. Fluorescence micrographs were acquired by an inverted laser scanning confocal microscope (Zeiss LSM 700), equipped with a 63× (1.4 NA) oil immersion objective.

Cell Migration Assay. A well-established *in vitro* scratch assay, proposed by Liang et al.,[36] was used to evaluate cell migration. This test is based on the observation that, upon creation of an artificial gap into a confluent cell monolayer, the cells on the edges of the gap move toward the open region to close the scratch until new cell−cell contacts are established again. It is reported that the cells initiate protrusion, migrate, and finally close the wound. Therefore, this assay evaluates the cell migration by estimating the speed of scratch healing, depending on the substrate.[37] The cells were seeded on *c*−, *c*+, and a glass slide as a control, with a density of 1×10^5 cells, and incubated at 37 °C in a 5% CO_2 atmosphere for 24 h, allowing the cells to adhere and grow until reaching ∼70−80% confluence as a monolayer. The cell monolayer was scraped after 24 h along a straight line, by using the plastic tip of a P200 pipet, to reduce as much as possible the damage to cells and substrate. Care has been taken in creating scratches of approximately similar size for each substrate to minimize any possible variation caused by the difference in the width of the scratches. The samples were washed twice in 1 mL of growth medium to remove debris and to smooth the scratch edges. The growth medium was replaced, and the dishes were placed back into the culture incubator. The samples were taken out of the incubator every 2 h to observe the scratch under an inverted microscope. The width of the scratch was measured as a function of time to determine the migration speed.

Statistical Analysis. The number of replicates for each experiment was adjusted according to the variance obtained. In graphs, all data were presented as means ± the standard deviation and evaluated for difference by a Student's *t* test. Differences were considered significant when $p < 0.05$.

RESULTS AND DISCUSSION

Cell Viability and Proliferation. Cells were seeded on the *c*+ and *c*− surfaces and observed under a standard inverted microscope at different time intervals, to gain a first view of their

DOI: 10.1021/acsami.5b05340
ACS Appl. Mater. Interfaces 2015, 7, 18113−18119

adhesion and proliferation onto the surface of LN crystals free of functionalization. Figure 1 reports the typical bright field images recorded over the 24 h.

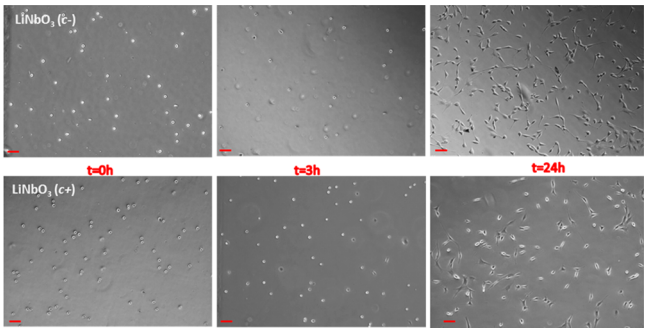

Figure 1. Typical bright field images of the cells seeded on *c*+ and *c*− free of functionalization and at the same time intervals (scale bar of 100 μm).

Cell spreading and adhesion appear to be similar on the two kinds of substrates, demonstrating the biocompatibility of the LN crystals in a first approximation. A more accurate evaluation of this biocompatibility was performed by the live/dead assay described previously, and Figure 2 shows the resulting fluorescence images.

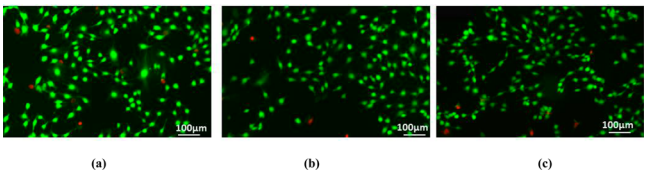

Figure 2. Typical fluorescence images of the cells seeded on (a) *c*−, (b) *c*+, and (c) glass, treated by the live/dead assay kit after incubation for 24 h.

The microscope observations showed a slightly, although not statistically significant, higher mortality for the cells seeded onto *c*+ than for those seeded onto *c*− and glass. The cells were then harvested and counted by a conventional Burker's chamber, and Figure 3 shows the proliferation rates.

Figure 4 shows the distributions of the live/dead cells over the different substrates after incubation for 24 and 48 h. The mean values for each substrate were evaluated over three biological replicates. The proliferation rate looks similar on the faces of LN and slightly higher than that on glass in the first 24 h, while negligible differences are observed after 48 h for all of the substrates. In fact, the population increases by ∼90% on LN faces and by ∼40% on glass, showing around 50% faster proliferation on LN, compared to glass in the first 24 h. This is in good agreement with the results reported by Carville et al.,[31] who found significant differences in osteoblast cell proliferation between *c*+ and *c*− were observed after incubation for only 6 days.

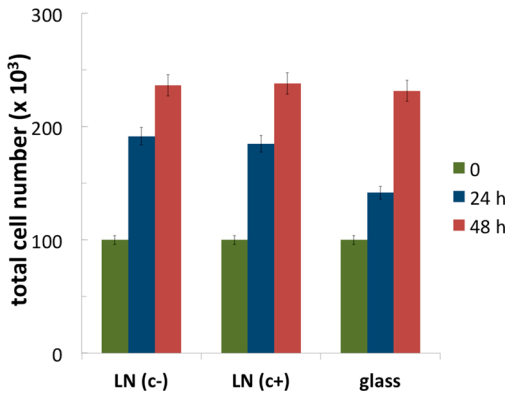

Figure 3. Cell growth on the three different substrates. Data are not statistically significant (*t* test; $p > 0.1$).

These results demonstrate that the surface of the LN crystals can be considered definitely biocompatible with negligible differences in cell mortality between *c*− and *c*+.

Morphology of Actin Filaments and Focal Adhesions. The adhesion and morphology of the cells were investigated via immunofluorescence analysis. Figure 5 shows the typical fluorescence images. The open source image processing program ImageJ, developed at the National Institutes of Health (NIH), was used to analyze the images.

The fluorescence images showed a non-negligible difference in the morphology of the actin filaments between the cells adhered on *c*− and *c*+, which is evidence of two classes of cells. The cells adhering on *c*+ showed a round-like morphology, a smaller size with a few irregular protrusions, and a marked decrease in the number of actin stress fibers. Conversely, the cells grown on *c*− exhibited a more elongated shape, with large spreading and more prominent stress fibers. The fibroblasts grown on *c*+ had poorly aligned stress fibers that could be viewed by fluorescence microscopy. In the case of negative polarity (*c*−), such actin fibers were a nearly universal feature of these cells. The less developed stress fibers observed on *c*+ were not an indication of toxicity, considering the results of the viability test reported previously. Moreover, the poor alignment of the stress fibers on *c*+ was more evident on more isolated cells. Figure 6 shows the typical case of confluent cells on *c*+, where the cells that made cell−cell contact frequently became elongated and developed stress fibers.

The more isolated cells in Figure 5 show an amorphous actin distribution with few stress fibers. Comparable cells on the same surface polarity that had made intercellular contact (see Figure 6) show the development of more stress fibers.

Multiple observations were made on different regions of the samples, and the ImageJ was used to count the cells that belong to the two classes of cell shape. Figure 7 shows quantitatively the dependence of the cell shape on the polarity of the LN surface.

Approximately 80% of the cells grown on *c*− showed a more elongated shape with well-aligned stress fibers. The examination of the focal adhesion formation on *c*+ and *c*− showed a significantly different morphology. After the cells had been plated for 24 h, the focal adhesions formed on *c*− were much larger than those formed on *c*+, as shown clearly in Figure 8.

The focal adhesions in cells plated on *c*− appeared elongated and oriented along the major cell axis, co-co-aligned with the stress fibers. Conversely, in the case of *c*+, the cells formed smaller and radially oriented focal adhesions with low aspect ratios.

Cell Migration. Figure 9 shows the typical bright field images of the scratch created on *c*−, *c*+, and a glass slide as a control, at equal time intervals.

Approximately 10 readings of the scratch width were considered for each sample at each observation time, and the mean values were calculated over three replicates of the experiments. Figure 10 shows the evolution of the scratch healing for the three substrates.

DOI: 10.1021/acsami.5b05340
ACS Appl. Mater. Interfaces 2015, 7, 18113−18119

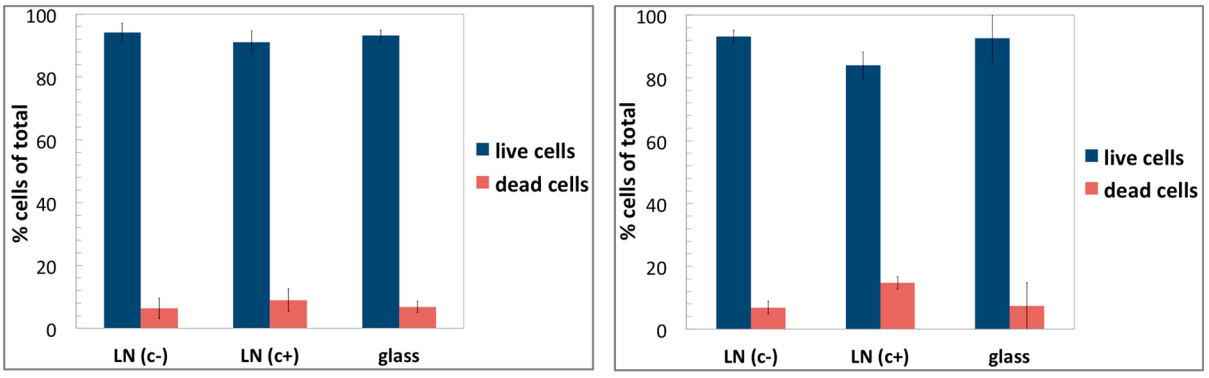

Figure 4. Distribution of the number of live/dead cells over the three substrates (glass, *c*−, and *c*+) after incubation for (a) 24 and (b) 48 h. The mean values were evaluated over three replicates of the experiment. Data are not statistically significant (*t* test; $p > 0.1$).

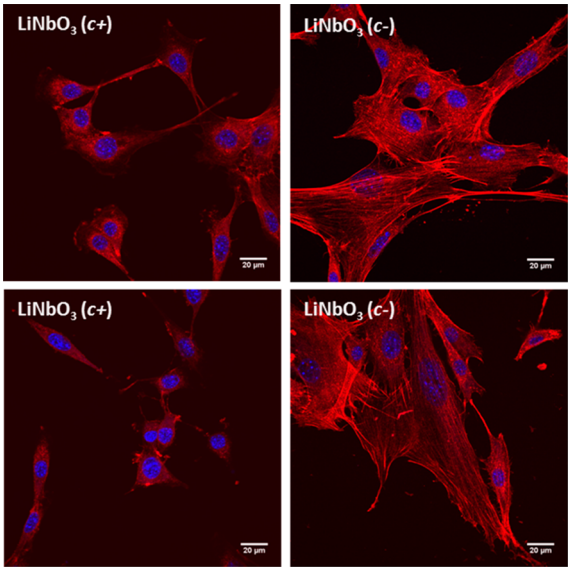

Figure 5. Confocal microscope images of cells seeded on *c*+ and *c*− after being cultured for 24 h, with nuclei and actin stained by DAPI (blue) and TRITC (red)-conjugated phalloidin, respectively.

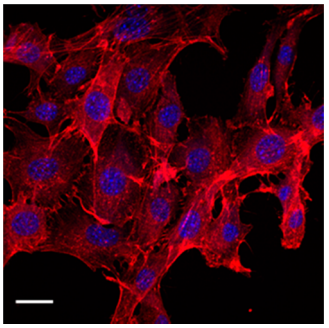

Figure 6. Confocal microscope image of confluent cells seeded on *c*+ and after incubation for 24 h, with nuclei and actin stained with DAPI and TRITC-conjugated phalloidin, respectively (scale bar of 20 μm).

The cell migration appeared to be clearly different for each substrate with faster scratch healing in the case of the *c*+ face. The cell layer advanced basically by spreading and translocation of existing cells. This is further indicated by the decrease in cell density as the layer advanced toward the wound and the increase in mean cell area at the wound edge. The increase in cell area

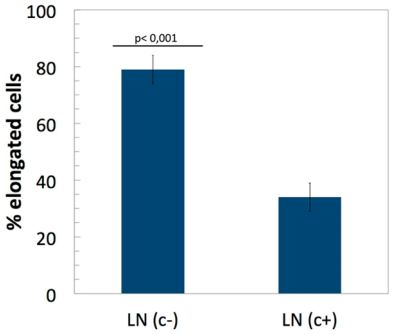

Figure 7. Distribution of the number of cells with a more elongated shape and aligned stress fibers. Statistical significance was evaluated by a Student's *t* test ($p < 0.001$).

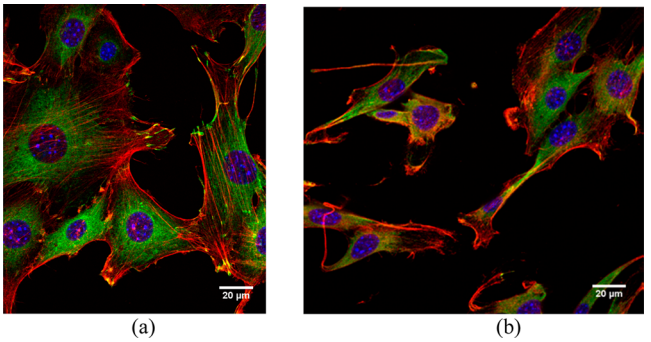

Figure 8. Confocal microscope images of cells plated (a) on the *c*− face and (b) on the *c*+ face and after incubation for 24 h, with nuclei, actin, and vinculin stained with DAPI, TRITC-conjugated phalloidin, and DyLight488 vinculin, respectively.

appeared to be significantly (only at 8 h) faster on *c*+, with ∼80% healing, compared to the value of 65% reached on *c*−. Lamellipodial protrusions are also known to guide cell migration.[38] During collective migration, cells at the wound edge and within the cell layer all actively migrate with lamellipodial protrusions extending mostly beneath adjacent cells, in the case of the inner cells, and toward the wound closure in the case of the edge cells. The cell protrusions in the closure region are prominent in the case of *c*+ (see Figure 9), in agreement with the faster wound healing exhibited by the measurements. The slowest scratch healing rate was obtained in the case of the glass slide, with ∼40% healing at the last point. These results demonstrate that the positive polarity of the

DOI: 10.1021/acsami.5b05340
ACS Appl. Mater. Interfaces 2015, 7, 18113−18119

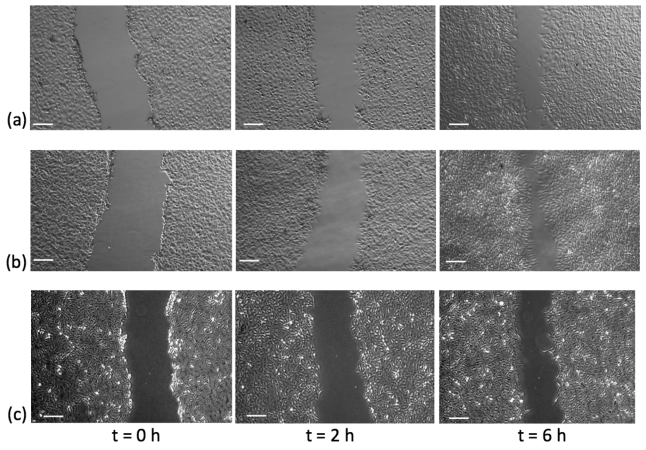

Figure 9. Typical optical microscope images of the evolution of the scratch over 6 h for (a) *c*−, (b) *c*+, and (c) a glass slide as a control (scale bar of 100 μm).

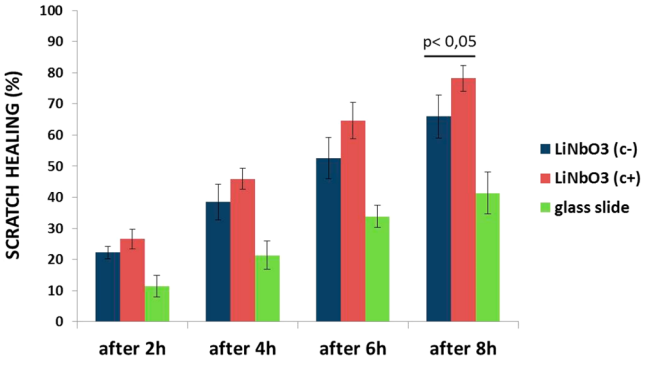

Figure 10. Percentage of scratch healing for each substrate. The mean values were calculated over three replicates of the experiments. The statistical significance was evaluated with a Student's *t* test ($p < 0.01$).

substrate increases significantly the speed of migration of the cells.

DISCUSSION

An early review by Davies[39] studied the importance of surface charges on cell behavior at the biomaterial interface and demonstrated that surface charges have a profound effect on biological responses. It was concluded that the surface charges affect the adsorption of proteins onto the material surface and subsequently influence the cell morphology and migration. Those conclusions were based on studies of cells cultured on charged polymer surfaces. This paper, instead, studies the *in vitro* response of fibroblast cells to the highest polarization magnitude of *c*-cut LN crystals ($P_s = 78\ \mu C/cm^2$), thus paving the way to an innovative platform for bioengineering applications. First, the biocompatibility of these crystals was assessed by standard viability assays. IUPAC (International Union of Pure and Applied Chemistry) defines biocompatibility as the "ability to be in contact with a living system without producing an adverse effect".[40] The results of the viability assays show that the LN crystals exhibit a biocompatible surface for the fibroblast cells. To the best of our knowledge, the interaction of the cell with the surface of these ferroelectric crystals has been explored poorly with only a couple of works presented in the literature very recently.[31,32] Christophis et al.[32] studied the adhesion of fibroblast cells onto polarized ferroelectric samples functionalized by a layer of fibronectin. They observed that the cells reoriented the position of their nuclei, avoiding the positions of high field gradients, without any additional observation about the morphology of the cells. Carville et al.[31] investigated the promotion of adhesion of osteoblasts and mineralization onto the surface of LN crystals, concluding that only the presence of charge played a role, but not the sign of the polarization. Other works deal with the bioactivity of LN and LT powders, but without any attention to the adhesion and morphology of the cells onto the crystal surface.[30] Conversely, different papers have been published in the past several years about the adhesion of osteoblastic cells to polarized ceramic substrates.[15,21−24] Therefore, today the literature lacks publications concerning the influence of the ferroelectric polarization on cell adhesion and morphology.

The results reported here demonstrate clearly that the surface polarity of the LN crystals has no significant effect on the proliferation rate of the adhered cells but, instead, has a substantial influence on the cell behavior in terms of morphology and migration. In fact, immunofluorescence analysis showed that the surface polarity induced remarkable differences in the arrangement of both cytoskeleton actin filaments and focal adhesions, and the migration assay demonstrated a significant difference in wound healing rate. The cells grown on *c*− presented a more pronounced spreading morphology, with well-aligned stress fibers and focal adhesions. This behavior could be explained by the differential adsorption of the chemical species floating into the culture medium. Figure 11 shows the schematic view of the mechanism proposed here for explaining how the exchange of environmental ions and proteins on *c*+ and *c*− may affect cell attachment.

The culture medium included different chemicals that had the same opportunity to interact and to be adsorbed on the surface of the crystal. However, the charged groups in the medium can be repulsed or attracted by the polarization charge on the crystal surface. Ca^{2+} ions are adsorbed predominantly on the negative

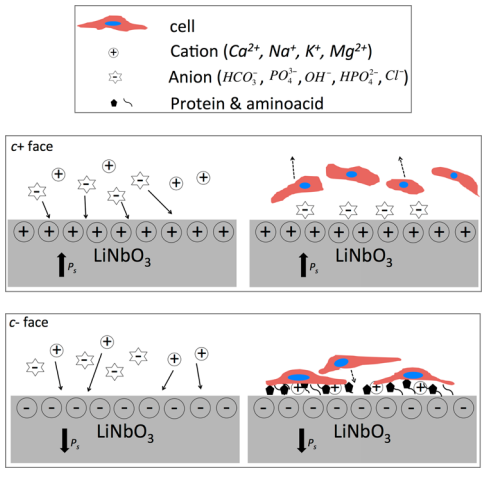

Figure 11. Schematic view of the interaction between the polarized surface of LN and the environmental species that contribute to cell adhesion. Organic and inorganic ions, amino acids, and proteins float around the crystal. Cations and positively charged ionic groups are actively adsorbed on the negatively charged surface (*c*−), thus contributing to the strong adhesion and spreading of the NIH-3T3 cells on this surface. Anions and negatively charged species are actively adsorbed on the positively charged surface (*c*+), thus reducing significantly the degree of cell spreading. The scheme is not to scale.

DOI: 10.1021/acsami.5b05340
ACS Appl. Mater. Interfaces 2015, 7, 18113−18119

polarity surface ($c-$) because of their superior binding affinity relative to the other cations in the medium, such as Na^+, K^+, and Mg^{2+}. The cell membrane comprises a negatively charged phospholipid bilayer with embedded proteins and sugars.[41] These groups show divalent cation-dependent ligand binding and form the well-known ECM, responsible for the cell adhesion behavior. Therefore, the abundant Ca^{2+} ions adsorbed on the $c-$ face tend to attract those cell adhesion proteins, thus promoting relatively strong cell adhesion. Conversely, the positive polarity of $c+$ tends to attract anionic groups, such as HPO_4^{2-} and/or HCO_3^{2-}, which have antiadhesive properties. This implies a weak link between the cell and the substrate because there are few points of interaction and attachment. Because the cell morphology is related closely to the cell adhesion force, the most important physiological result of this different interaction between ions, cell adhesion proteins, and polarized surface is the different morphology and assembly of the stress fibers and focal adhesions. The cells assume a flat morphology, and the adhesion plaque is extensive when a strong adhesion force is exerted on the ECM. This is the case for $c-$, where a major concentration of cations makes a stable and heavy link between the cell and the substrate, thus producing a significant formation and maintenance of well-aligned stress fibers and mainly peripheral focal adhesions. This implies that cells possessed better cell−substrate interaction to promote growth. Conversely, the cells primarily have a spherical shape and do not exert a great adhesion force on the matrix when poor attachment force exists. This is the case of $c+$, where the cells have smaller focal adhesions and poorly oriented actin networks. The vinculin expression had a relatively sparse distribution around the nuclei, meaning that fibroblasts spread less and had less traction force for anchoring onto the substrate.[42] This weaker adhesion explains the prominent concrete and solid shape of the cells grown on $c+$.[43−45]

The predominant well-organized stress fibers and peripheral focal adhesions on $c-$, observed in our research, are in agreement with the results concerning the cell migration rate. In fact, recent studies have reported that stress fibers are abundant and well-structured when cell adhesion is promoted and, conversely, they are absent or not well-structured in the case of many highly motile cells, such as leukocytes.[46] This may explain the higher wound healing rate observed in cells grown on $c+$, where the predominant adsorption of anionic groups tends to weaken the cell adhesion in favor of increased motility. The availability of an innovative functional material able to control the cell migration through surface charge is of great interest in different fields of application, to understand better the role of polarity in cell functions related to migration behavior. In fact, cell migration plays a central role in diverse biological phenomena, including the ability of the cell to answer to particular chemical or mechanical stimuli. For example, cell migration is crucial during development and wound healing.[38,47] In fact, a well-controlled cell migration is associated with normal development and function, while a misregulated motility potentiates a multitude of pathologies, including inflammation and cancer metastasis. Cell migration is also essential for technological processes that concern the tissue engineering applications, where it is of crucial importance for colonizing the biomaterial scaffold. Not surprisingly, a variety of cell migration assays have been designed to investigate the critical components that control cell movement.[48]

It is noteworthy that, different from the conclusions drawn by Carville et al.,[31] the findings presented here about the stronger adhesion of fibroblasts on $c-$ are in agreement with previous studies by Kizuki et al.,[24] who reported how the higher cell affinity of the negative face of polarized ceramics was caused by its ability to recruit the Ca^{2+} ions present in the culture medium, thus confirming such an interpretation.

CONCLUSION

Cell behavior was investigated by cell culture on c-cut LN crystals. Here, for the first time, significant differences in cell behavior were observed on the faces of LN crystals with opposite polarities. In particular, stronger cell adhesion with good alignment of stress fibers and focal adhesions were found in the case of the negative face ($c-$). Moreover, the consequent influence on cell migration was revealed by standard assays that showed a higher wound healing rate on $c+$, in full agreement with well-established studies that show how stronger cell adhesion is always associated with low-motility cells. The overall results demonstrate that, contrary to a couple of works published recently on this topic, the LN crystals can be definitely used as an innovative platform for manipulating cells thorough the effects of its high-magnitude spontaneous polarization, thus opening the way to the development of new principles that can be used for tissue engineering applications. In fact, compared to standard biomaterials, this kind of platform could provide revolutionary integrated functionalities than can modulate the cell response through the surface charge patterning in combination with key properties that include pyroelectricity, photorefractivity, and optical nonlinearity.

AUTHOR INFORMATION

Corresponding Author

*E-mail: simonetta.grilli@cnr.it.

Author Contributions

V.M. and O.G. contributed equally to this work.

Notes

The authors declare no competing financial interest.

ACKNOWLEDGMENTS

We acknowledge the Italian Ministry of Research for financial support under “Futuro in Ricerca 2010” Programme (Protocol RBFR10FKZH) and under the “Progetto Operativo Nazionale” AquaSystem (Protocol 1719).

REFERENCES

(1) Anderson, J. M. Biological Responses to Materials. *Annu. Rev. Mater. Res.* **2001**, *31*, 81−110.
(2) Sakiyama-Elbert, S. E.; Hubbell, J. A. Functional Biomaterials: Design of Novel Biomaterials. *Annu. Rev. Mater. Res.* **2001**, *31*, 183−201.
(3) Seal, B. L.; Otero, T. C.; Panitch, A. Polymeric Biomaterials for Tissue and Organ Regeneration. *Mater. Sci. Eng., R* **2001**, *34*, 147−230.
(4) Levenberg, S.; Langer, R. Advances in Tissue Engineering. *Curr. Top. Dev. Biol.* **2004**, *61*, 113−34.
(5) Anderson, D. G.; Burdick, J. A.; Langer, R. MATERIALS SCIENCE: Smart Biomaterials. *Science* **2004**, *305*, 1923−1924.
(6) Temenoff, J. S.; Mikos, A. G. Reviews: Tissue Engineering for Regeneration of Articular Cartilage. *Biomaterials* **2000**, *21*, 431−40.
(7) Chen, H.; Yuan, L.; Song, W.; Wu, Z.; Li, D. Biocompatible Polymer Materials: Role of Protein−Surface Interactions. *Prog. Polym. Sci.* **2008**, *33*, 1059−1087.
(8) Pankov, R.; Yamada, K. M. Fibronectin at a Glance. *J. Cell Sci.* **2002**, *115*, 3861−3863.
(9) Ehrenberg, M. S.; Friedman, A. E.; Finkelstein, J. N.; Oberdorster, G.; McGrath, J. L. The Influence of Protein Adsorption on Nanoparticle

DOI: 10.1021/acsami.5b05340
ACS Appl. Mater. Interfaces 2015, 7, 18113−18119

Association with Cultured Endothelial Cells. *Biomaterials* **2009**, *30*, 603−610.
(10) Calatayud, M. P.; Sanz, B.; Raffa, V.; Riggio, C.; Ibarra, M. R.; Goya, G. F. The Effect of Surface Charge of Functionalized Fe_3O_4 Nanoparticles on Protein Adsorption and Cell Uptake. *Biomaterials* **2014**, *35*, 6389−6399.
(11) Lin, S.; Huang, S.; Chen, S.; Vinzons, L. U.; Ciou, J.; Wong, P. Investigation of the Interfacial Effects of Small Chemical-Modified TiO_2 Nanotubes on 3T3 Fibroblast Responses. *ACS Appl. Mater. Interfaces* **2014**, *6*, 12071−12082.
(12) Manshian, B. B.; Moyano, D. F.; Corthout, N.; Munck, S.; Himmelreich, U.; Rotello, V. M.; Soenen, S. J. High-Content Imaging and Gene Expression Analysis to Study Cell - Nanomaterial Interactions: The Effect of Surface Hydrophobicity. *Biomaterials* **2014**, *35*, 9941−9950.
(13) Shiu, J.; Kuo, C.; Whang, W.; Chen, P. Observation of Enhanced Cell Adhesion and Transfection Efficiency on Superhydrophobic Surfaces. *Lab Chip* **2010**, *10*, 556−558.
(14) Lin, J.; Chang, H.; Kao, W.; Lin, K.; Liao, H.; You, Y.; Kuo, Y.; Kuo, D.; Chu, K.; Chu, Y.; Shyue, J. Effect of Surface Potential on Extracellular Matrix Protein Adsorption. *Langmuir* **2014**, *30*, 10328−10335.
(15) Baxter, F. R.; Bowen, C. R.; Turner, I. G.; Dent, A. C. E. Electrically Active Bioceramics: A Review of Interfacial Responses. *Ann. Biomed. Eng.* **2010**, *38*, 2079−2092.
(16) Fukada, E.; Yasuda, I. On the Piezoelectric Effect of Bone. *J. Phys. Soc. Jpn.* **1957**, *12*, 1158−1162.
(17) Hastings, G. W.; Mahmud, F. A. The Electromechanical Properties of Fluid-Filled Bone: a New Dimension. *J. Mater. Sci.: Mater. Electron.* **1991**, *2*, 118−124.
(18) McElhaney, J. H. The Charge Distribution on the Human Femur Due to Load. *J. Bone. Jt. Surg.* **1967**, *49A*, 1561−1571.
(19) Feng, J.; Yuan, H. P.; Zhang, X. D. Promotion of Osteogenesis by a Piezoelectric Biological Ceramic. *Biomaterials* **1997**, *18*, 1531−1534.
(20) Kobayashi, T.; Nakamura, S.; Yamashita, K. Enhanced Osteobonding by Negative Surface Charges of Electrically Polarized Hydroxyapatite. *J. Biomed. Mater. Res.* **2001**, *57*, 477−484.
(21) Nakamura, M.; Nagai, A.; Tanaka, Y.; Sekijima, Y.; Yamashita, K. Polarized Hydroxyapatite Promotes Spread and Motility of Osteoblastic Cells. *J. Biomed. Mater. Res., Part A* **2010**, *92A*, 783−790.
(22) Ohgaki, M.; Kizuki, T.; Katsura, M.; Yamashita, K. Manipulation of Selective Cell Adhesion and Growth by Surface Charges of Electrically Polarized Hydroxyapatite. *J. Biomed. Mater. Res.* **2001**, *57*, 366−373.
(23) Nakamura, M.; Sekijima, Y.; Nakamura, S.; Kobayashi, T.; Niwa, K.; Yamashita, K. Role of Blood Coagulation Components as Intermediators of High Osteoconductivity of Electrically Polarized Hydroxyapatite. *J. Biomed. Mater. Res., Part A* **2006**, *79*, 627−634.
(24) Kizuki, T.; Ohgaki, M.; Katsura, M.; Nakamura, S.; Hashimoto, K.; Toda, Y.; Udagawa, S.; Yamashita, K. Effect of Bone-Like Layer Growth From Culture Medium on Adherence of Osteoblast-Like Cells. *Biomaterials* **2003**, *24*, 941−947.
(25) Israelachvili, J. *Intermolecular and Surface Forces*, 2nd ed.; Academic Press: San Diego, 2000; p 217.
(26) Zhang, A.; Sharma, P.; Borca, C. N.; Dowben, P. A.; Gruverman, A. Polarization-Specific Adsorption of Organic Molecules on Ferroelectric $LiNbO_3$ Surfaces. *Appl. Phys. Lett.* **2010**, *97*, 243702−3.
(27) Dunn, S.; Cullen, D.; Abad-Garcia, E.; Bertoni, C.; Carter, R.; Howorth, D.; Whatmore, R. W. Using the Surface Spontaneous Depolarization Field of Ferroelectrics to Direct the Assembly of Virus Particles. *Appl. Phys. Lett.* **2004**, *85*, 3537−3.
(28) Garra, J.; Vohs, J. M.; Bonnell, D. A. The Effect of Ferroelectric Polarization on the Interaction of Water and Methanol with the Surface of $LiNbO_3$(0001). *Surf. Sci.* **2009**, *603*, 1106−1114.
(29) Sun, X.; Su, Y. J.; Li, X.; Gao, K. W.; Qiao, L. J. Stability of Nano-Scale Ferroelectric Domains in a $LiNbO_3$ Single Crystal: the Role of Surface Energy and Polar Molecule Adsorption. *J. Appl. Phys.* **2012**, *111*, 094110−6.
(30) Vilarinho, P. M.; Barroca, N.; Zlotnik, S.; Félix, P.; Fernandes, M. H. Are Lithium Niobate ($LiNbO_3$) and Lithium Tantalate ($LiTaO_3$) Ferroelectrics Bioactive? *Mater. Sci. Eng., C* **2014**, *39*, 395−402.
(31) Carville, N. C.; Collins, L.; Manzo, M.; Gallo, K.; Lukasz, B. I.; McKayed, K. K.; Simpson, J. C.; Rodriguez, B. J. Biocompatibility of Ferroelectric Lithium Niobate and the Influence of Polarization Charge on Osteoblast Proliferation and Function. *J. Biomed. Mater. Res., Part A* **2015**, *103*, 2540−2548.
(32) Christophis, C.; Cavalcanti-Adam, E. A.; Hanke, M.; Kitamura, K.; Gruverman, A.; Grunze, M.; Dowben, P. A.; Rosenhahn, A. Adherent Cells Avoid Polarization Gradients on Periodically Poled $LiTaO_3$ Ferroelectrics. *Biointerphases* **2013**, *8*, 27−35.
(33) Weis, R. S.; Gaylord, T. K. Lithium Niobate: Summary of Physical Properties and Crystal Structure. *Appl. Phys. A: Solids Surf.* **1985**, *37*, 191−203.
(34) Ryoo, S. R.; Kim, Y. K.; Kim, M. K.; Min, D. H. Behaviours of NIH-3T3 Fibroblasts on Graphene/Carbon Nanotubes: Proliferation, Focal Adhesion, and Gene Transfection Studies. *ACS Nano* **2010**, *4*, 6587−6598.
(35) Dolatshahi-Pirouz, A.; Jensen, T.; Kraft, D. C.; Foss, M.; Kingshott, P.; Hansen, J. L.; Larsen, A. N.; Chevallier, J.; Besenbacher, F. Fibronectin Adsorption, Cell Adhesion, and Proliferation on Nanostructured Tantalum Surfaces. *ACS Nano* **2010**, *4*, 2874−2882.
(36) Liang, C.; Park, A. Y.; Guan, J. In Vitro Scratch Assay: a Convenient and Inexpensive Method for Analysis of Cell Migration in Vitro. *Nat. Protoc.* **2007**, *2*, 329−333.
(37) Yarrow, J. C.; Perlman, Z. E.; Westwood, N. J.; Mitchison, T. J. A High-Throughput Cell Migration Assay Using Scratch Wound Healing, a Comparison of Image-Based Readout Methods. *BMC Biotechnol.* **2004**, *4*, 21−29.
(38) Ridley, A. J.; Schwartz, M. A.; Burridge, K.; Firtle, R. A.; Ginsberg, N. H.; Borisy, G.; Parsons, J. T.; Horwitz, R. Cell Migration: Integrating Signals from Front to Back. *Science* **2003**, *302*, 1704−1709.
(39) Davies, J. E. The Importance and Measurement of Surface Charge Species in Cell Behaviour at the Biomaterial Interface. *Surface Characterisation of Biomaterials*, 1988.
(40) Vert, M.; Doi, Y.; Hellwich, K.; Hess, M.; Hodge, P.; Kubisa, P.; Rinaudo, M.; Schué, F. Terminology for Biorelated Polymers and Applications (IUPAC Recommendations 2012). *Pure Appl. Chem.* **2012**, *84*, 377−410.
(41) Healy, K. E.; Lom, B.; Hockberger, P. E. Spatial Distribution of Mammalian Cells Dictated by Material Surface Chemistry. *Biotechnol. Bioeng.* **1994**, *43*, 792−800.
(42) Dumbauld, D. W.; Lee, T. T.; Singh, A.; Scrimgeour, J.; Gersbach, C. A.; Zamir, E. A.; Fu, J.; Chen, C. S.; Curtis, J. E.; Craig, S. W.; García, A. J. How Vinculin Regulates Force Transmission. *Proc. Natl. Acad. Sci. U. S. A.* **2013**, *110*, 9788−9793.
(43) Mattila, P. K.; Lappalainen, P. Filopodia: Molecular Architecture and Cellular Functions. *Nat. Rev. Mol. Cell Biol.* **2008**, *9*, 446−454.
(44) Yeung, T.; Georges, P. C.; Flanagan, L. A.; Marg, B.; Ortiz, M.; Funaki, M.; Zahir, N.; Ming, W.; Weaver, V.; Janmey, P. A. Effects of Substrate Stiffness on Cell Morphology, Cytoskeletal Structure, and Adhesion. *Cell Motil. Cytoskeleton* **2005**, *60*, 24−34.
(45) Pellegrin, S.; Mellor, H. Actin Stress Fibres. *J. Cell Sci.* **2007**, *120*, 3491−3499.
(46) Valerius, N. H.; Stendahl, O.; Hartwig, O. X.; Stossel, T. P. Distribution of Actin-Binding Protein and Myosin in Polymorphonuclear Leukocytes. *Cell* **1981**, *24*, 195−202.
(47) Gilbert, S. F. *Developmental Biology*, 7th ed.; Sinauer: Sunderland, MA, 2003.
(48) Kramer, N.; Walzl, A.; Unger, C.; Rosner, M.; Krupitza, G.; Hengstschlager, M.; Dolznig, H. In Vitro Cell Migration and Invasion Assays. *Mutat. Res., Rev. Mutat. Res.* **2013**, *752*, 10−24.

DOI: 10.1021/acsami.5b05340
ACS Appl. Mater. Interfaces 2015, 7, 18113−18119